

## Semi-automatic analysis of microscopic images of the human cerebral cortex using the grey level index

by BERNWARD SAUER, *Department of Neuroanatomy, Medical School of Hannover, Karl-Wiechert-Allee 9, D-3000 Hannover 61, F.R.G.*

KEY WORDS. Automatic data processing, cerebral cortex, human, cytoarchitectonics, striate area, grey level index profile.

### SUMMARY

A new semi-automatic method is introduced which makes possible the quantitative examination of cresyl-fast-violet stained sections of the cerebral cortex. These sections are divided into measuring fields of  $20 \times 20 \mu\text{m}$  in a well-defined area. A scanning procedure then automatically determines the grey level index of every single field. The image of the histological section can be compared with the grey level index data matrix by means of a plotted image, the density of the plotted points of which is proportional to the measured grey level index. By overlaying this plotted image with the original section, the boundaries of the laminae can be fixed in the data matrix. The grey level index profiles—the grey level data plot as a function of the cortical depth—after smoothing and standardization are typical of special cortical areas. The mean thickness and the mean portion of the grey level index profile of the different laminae of the striate area are compared with data from other publications.

### INTRODUCTION

Quantitative analysis of cytological parameters of cortical areas of the human brain depends on a wide range of methodical factors. The thickness of a section, for example, influences the measurement of the cell density. Another essential problem of all quantitative examinations, in view of cytoarchitecture, is the resultant enormous amount of data, particularly the considerable time required for its recording and evaluation.

A further disadvantage of quantitative methods in biology and medicine is the individuality of each organism, which gives rise to great variations in measured data. This considerably limits the validity of a single measurement and only an examination of a great number of individuals from a population, together with a follow-up statistical evaluation, will give reproducible results. However, this process is very time-consuming.

Modern computers offer a simple solution to these problems. Furthermore, if the actual measurement process can be undertaken by an automatic image analyser, a very time-saving method for quantitative studies of microscopic images will be at one's disposal.

In recent years, automatic measurements in medicine and biology employing image analysis systems and photometers together with computers have mainly been used for analysing microstructures such as single cells or cell-elements (Wied *et al.*, 1978; Tucker, 1979). This paper describes a new method which permits semi-automatic analysis of laminated biological structure. The technique is applied to stained sections of the human cerebral cortex, in particular to the striate area of normal adult brains. In principle, however, it is possible to use this method to

analyse many two- and three-dimensional laminated structures, such as bone tissue, skin, bowel, etc.

When using an automatic measuring method, the capabilities of the image analyser must be taken into account. A useful parameter is the grey level index (GLI) defined by Schleicher *et al.* (1978) which has already been used successfully for demarcating and describing brain areas (Zilles *et al.*, 1980) and for analysing laminated structures of the striate area (Zilles & Schleicher, 1980).

#### MATERIAL

Eleven brains were selected as being normative according to the following criteria: adult brains not older than 60 years, no cerebral causes of death, no neurological or psychiatric diseases, and no pathological findings. Blocks of striate area of about 2/2 cm in size were cut from the cortex of formalin-fixed brains and embedded in paraffin. These blocks were cut into sections 10–40  $\mu\text{m}$  thick using a Leitz-Mikrotome, and were alternately stained with cresyl-fast-violet according to Nissl, silver-impregnated and myelin sheath stained. Some eight to twelve sections per brain were used for quantitative analyses to reduce the influence of intra-individual variability.

#### METHOD

##### *Measuring equipment*

The layout of the technical equipment is shown in Fig. 1. An image analyser (Microvideomat II, Zeiss, Oberkochen) is used to calculate the GLI from an image signal picked up by a television camera. This camera receives the contents of the image from the beam of a microscope (Zeiss Photomicroscope) with a scanning stage. A photomicroscope with a Planapo 63/1.4 oil immersion objective, a 1.3-fold aperture and a twofold optovar is used, which enables a photograph to be taken before every measurement of the analysed cortex part; this is of great import-

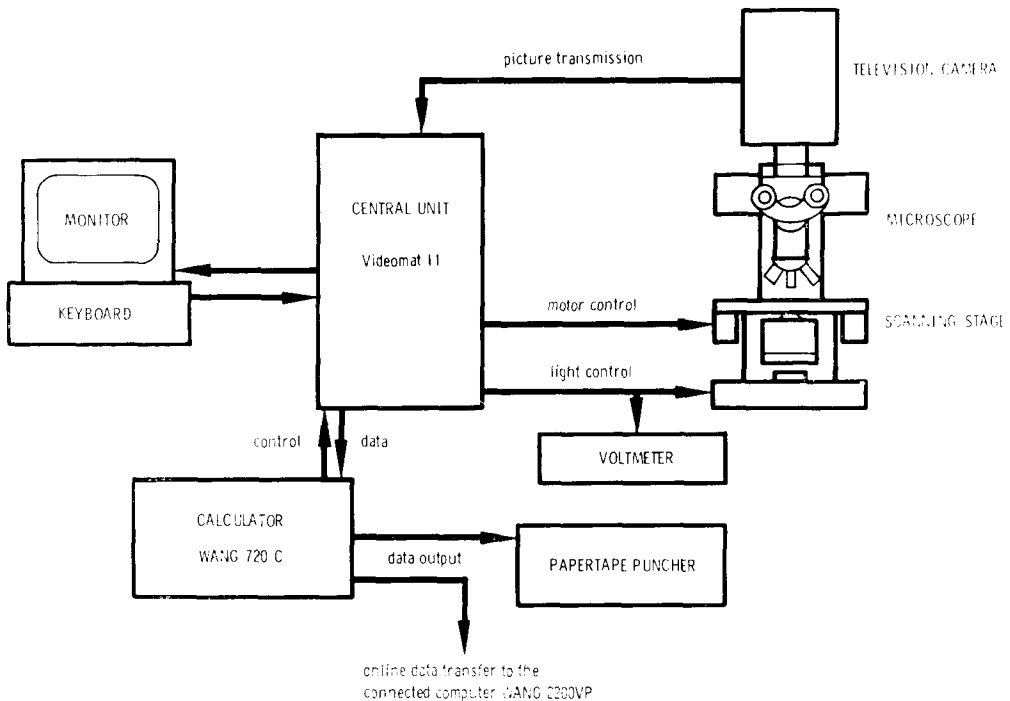


**Fig. 1.** Schematic arrangement of the equipment for the automatic measuring method.

ance for the later retrieval of the examined part. The complete system is controlled by a programmable calculator (Wang 720C). The data recalled from the image analyser are either punched out on paper tape or fed into a computer by online data transmission. This computer (Wang 2200 VP) evaluates the data obtained from the measuring equipment described above and shows the results on a graphic display.

*Aspects of quantification:*

The described equipment enables the measurement of cresyl-fast-violet stained cortical sections of the human brain. Each section is divided into a grid-like arrangement of measuring fields (Fig. 2) (Schleicher *et al.*, 1978; Zilles *et al.*, 1978) and the GLI is determined for every field. The threshold of the image analyser should be adjusted in such a way that the GLI essentially indicates the projected area of those stained neurons in a measured field which are visible in the area of depth of focus of the microscope. If the edges of the measured fields are exactly parallel and vertical to the surface of the cortex, one value for one row can be obtained by adding and calculating the mean value of this row (the rows should be parallel and the columns vertical to the surface of the brain). If the same procedure is undertaken for all rows and if the resulting GLI-data are plotted as a function of cortical depth (the distance to the cortical

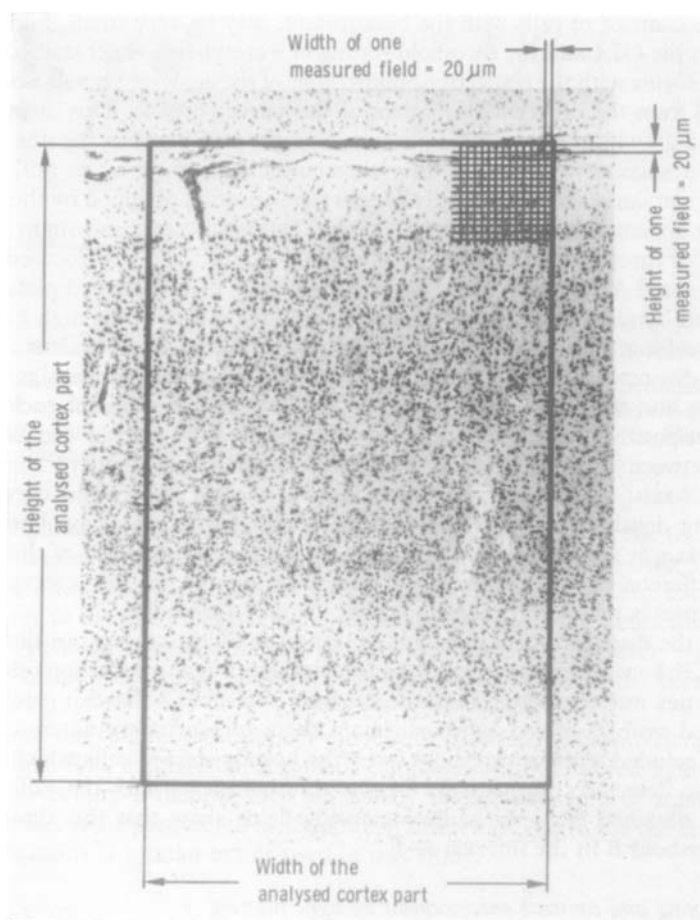


**Fig. 2.** Microphotograph of the striate area (20  $\mu\text{m}$  serial section, cresyl-fast-violet staining). The analysed cortex part is demarcated and partially divided into measuring fields 20  $\times$  20  $\mu\text{m}$  in size. The GLI is determined for every measuring field by the instruments shown in Fig. 1.

surface), a GLI profile of the cortex of the examined section will be obtained. If the GLIs of the rows of a cortical structure (i.e. one lamina) are summarized in a certain way, the result of the described procedure is one value for one structure. Thus, different structures can be compared with one another as well as with the same structures of other parts of the cortex.

#### *Grey level index*

The central parameter in the following method is the grey level index (GLI). This is defined as the fraction (in per cent) of a specific image area, the grey level of which lies below a fixed threshold. This threshold is to set essentially to include the neurons. The image analyser used can only detect stained structures which differ from the background by a higher grey level. As cresyl-fast-violet mainly stains the nucleic acids, the nuclei of glia, neurons and pial and endothelial cells as well as the RNA-containing perikarya of the neurons are included. The areal extension of all latter structures correspond with the GLI. Presupposing that small vessels are randomly distributed and the areal fraction of glia nuclei is small, the differences in the GLI arise mainly from the total amount of neurons in the measured field. The influence of large vessels, resulting in a high GLI at this point, can be eliminated by selecting a cortical part without any larger vessels for the final analysis.

If quantitative measurements are to be reproducible, it is important that the grey threshold is set in a well-defined way. Since biological structures are not homogeneous, the intensity of staining, i.e. the contrast of cells with the background, may be very small. Figure 3 shows the relation between the GLI and the threshold setting of a cresyl-fast-violet stained section of the human cerebral cortex with the respective photographs of the analyser screen. Better information can be obtained from the differential quotient of this curve (Fig. 4). This differential quotient curve, also called grey level histogram, indicates the difference between the number of detected picture points at successive optical density thresholds. Robertson *et al.* (1978) used such a differential quotient curve (calling it optical density/area profile) obtained by the Quantimet 720 image analysing system to grade cerebral gliomas. The first increase and slight decrease of this curve to the left of threshold A is caused by intensively-stained and well-focused structures. To the right of threshold A, the curve runs through an even to trough-shaped plateau (A-B). This interval is caused by cells which are no longer so well-focused having a high grey level as well as less light-absorbing, well-focused cell particles. At threshold B, an evident turn is seen and the curve rises distinctly. Here the detection of the background becomes significant. If GLI-threshold-curves and their derivatives (Fig. 4) for cortex parts of different packing densities of cresyl-fast-violet-positive structures are compared, the typical plateau can be recognized in every curve. Between threshold A and B, the three differential quotient curves run almost parallel to the *x*-axis. In this discrimination interval the GLI/threshold curves (Fig. 3) for different packing densities of stained structures can be approximated by lines which almost intersect the *x*-axis at one point. However, this means that the relation of the GLIs between images with different packing densities of stained structures in this interval (A-B) in one selected cortex part is practically independent of the grey-threshold.

In practice, the discrimination threshold is set in the following way. In the selected cortex part in which GLI-measurements are to be undertaken, a few measuring fields with average nerve-cell-densities were chosen. The discrimination threshold is fixed in such a way that all well-focused and visibly stained cell-particles in these measuring fields are detected and no background is included. At this threshold level, the heavily stained cells which are slightly out of focus are also detected. Comparisons of this threshold-level with the differential quotient curves (Fig. 4) obtained from the same measuring fields show that this threshold is usually placed near threshold B in the interval A-B.

#### *Influence of staining and contrast enhancement by light filtering*

Since all sections are stained by the same procedure, differences of section staining should be negligible. Above all, in one analysed cortex part of a section, which is only about  $1 \times 2$  mm in size, no staining differences are to be expected. Nevertheless, apparent staining differences of

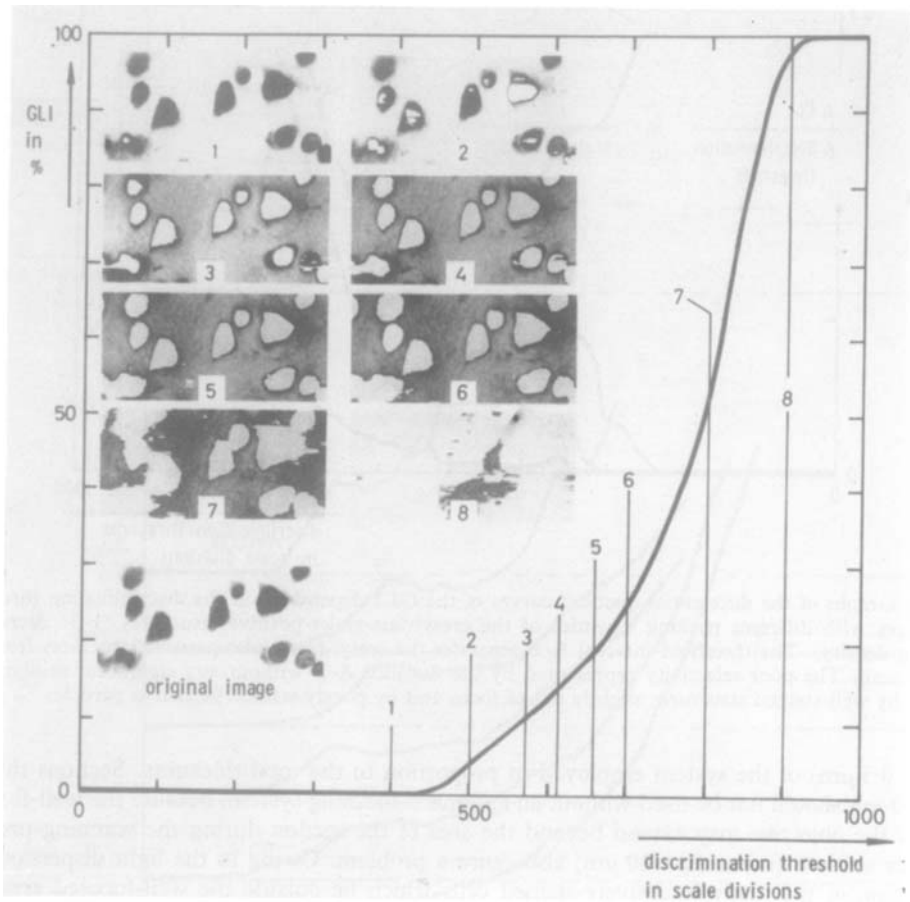


**Fig. 3.** GLI and the discrimination threshold. The grey level index is 0% on discrimination threshold 0 (=black) and 100% on discrimination threshold 1000 (=white). The increasing curve indicates the amount of detected picture points at any discrimination threshold. Monitor images of the Micro-Videomat are shown at different thresholds (the light areas represent the detected image-parts).

different sections influence the shape of the differential quotient curve of the measuring field of the section in question. In heavily stained sections, the threshold for detecting the stained particles shifts to a lower level. Thus, the level for these particles and the background move apart and the curve in the threshold interval A–B decreases and forms a minimum. This means that the contrast between stained cells and background increases. However, when setting the threshold in the manner described above, it is always placed between the threshold levels A and B of this section.

Figure 5 shows the differential quotient curves for different filter-wavelengths compared with unfiltered light. The contrast enhancement compared with unfiltered light is represented by a wide plateau behind a distinct increase caused by the detection of intensively stained particles. 550 nm has to be considered as an optimal filter-wavelength for the cresyl-fast-violet stained cortical sections of human brains used in this study.

#### *Thickness of the section*

The thickness of cortical sections generally used in this study is 20  $\mu\text{m}$ . However, the method can also be applied to other thicknesses of sections (10–40  $\mu\text{m}$ ), because the total thickness of sections in this range does not influence the results. This is due to the very small focal depth

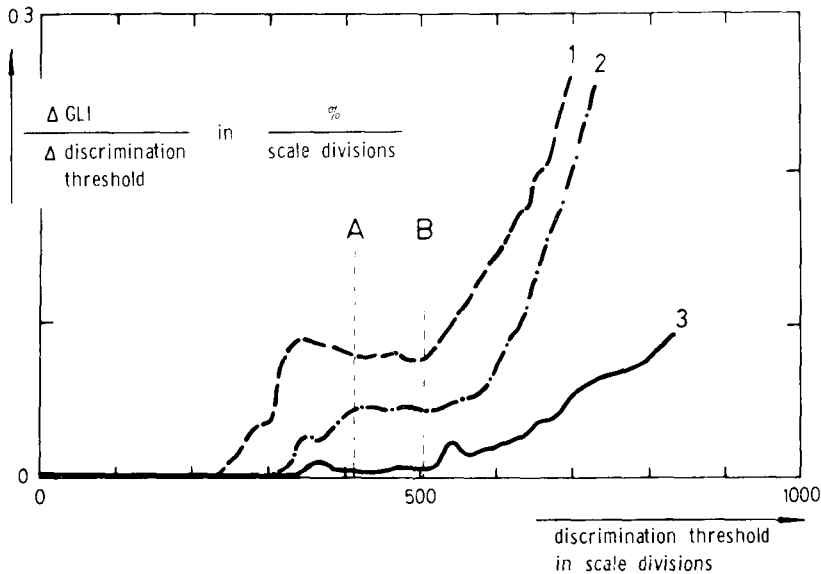


**Fig. 4.** Graphs of the differential quotient curves of the GLI dependent on the discrimination threshold of images with different packing densities of the cresyl-fast-violet-positive structures (1–3: decreasing packing density). The threshold-interval A–B separates the cresyl-fast-violet-positive structures from the background. The poor selectivity represented by the distance A–B without any significant minimum is caused by well-stained structures slightly out of focus and by poorly stained perikarya particles.

(about  $0.5 \mu\text{m}$ ) of the system employed in proportion to the total thickness. Sections thinner than  $10 \mu\text{m}$  should not be used without an automatic focusing system, because the well-focused area of the objective may extend beyond the area of the section during the scanning-process. Thicker sections (more than  $40 \mu\text{m}$ ) also cause a problem. Owing to the light dispersion and absorption of the many intensively-stained cells which lie outside the well-focused area, the background of areas which are crowded with stained cells will be considerably darker than the background which is lacking in cells. Thus, for such cell-dense fields, the discrimination threshold between a well-focused cell and the background shifts to darker grey levels. There is then the risk that the GLIs of the areas of high cell densities will be overestimated.

#### *Measuring process control*

For quantitative examination of the human cerebral cortex, each measured field should be  $20/20 \mu\text{m}$  in size. This represents a compromise between high resolution and rapid measurement. One considerable period of time is that between the resetting of the scanning stage on to a new measuring field and the recall of the measured data from the analyser. The calculating time for data manipulations and process-controlling per single field is also considerable.

Using the period between resetting and recall for processing the data of the previous measurement, the total measuring time for one section could almost be halved. It was further reduced by a time-efficient programming of the calculator controlling the measuring process. Thus, nearly 7000 measuring fields can be measured every 10 min.

#### *Plotted image*

An essential aim of the examination of human cerebral cortex is to produce quantitative data on a single lamina. Exact demarcation of the laminae is only possible on the original slide using a microscope. Therefore, at this point of the analysis process, human decision by the investigator is necessary. The idea of the plotted image is to form a connection between the original image and the GLI-data matrix. Thus, the data matrix is reconverted into a black and white image by

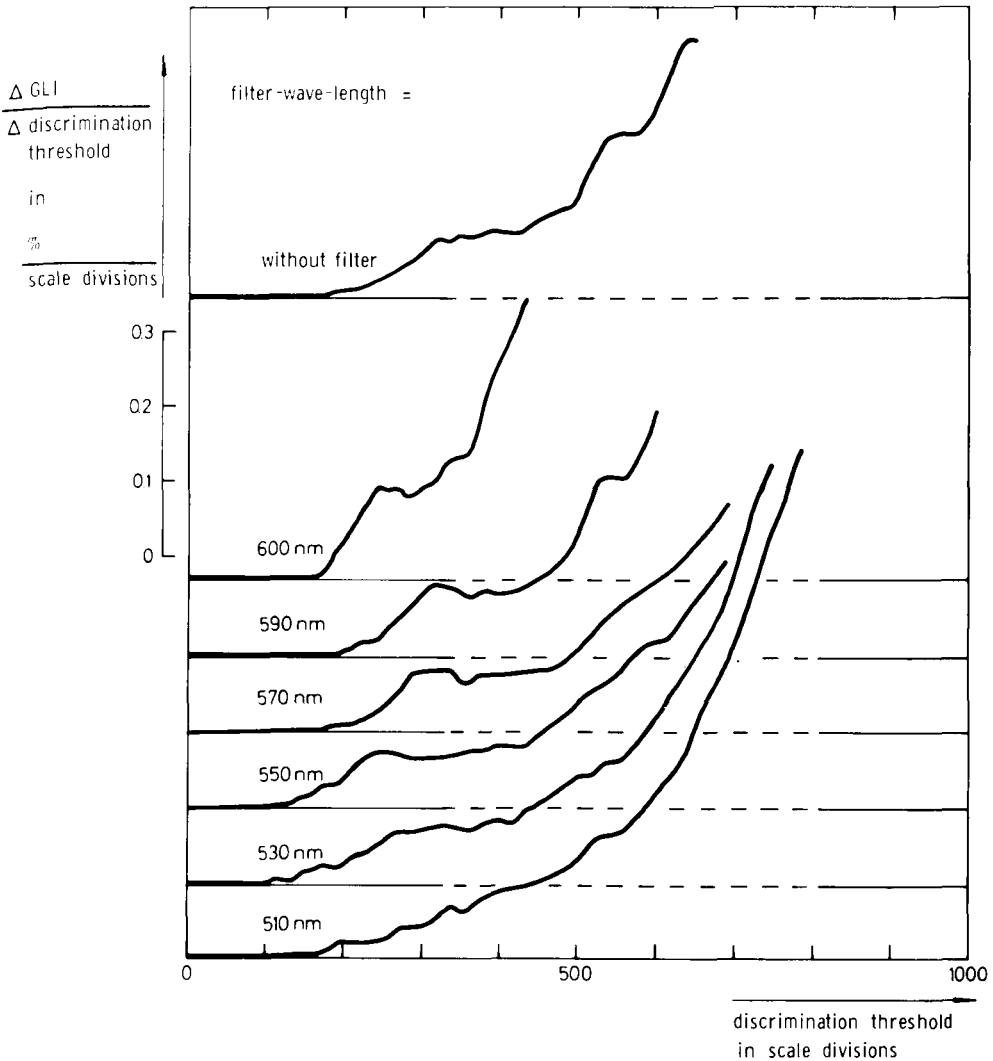


**Fig. 5.** Graphs of the differential quotient curves of the GLI dependent on the discrimination threshold using filters with different wavelengths in contrast to unfiltered light. Contrast enhancement is indicated by a wide distance between the first significant increase or peak in the left and the distinct increase in the right and a plateau or trough-shaped running of the curve in the latter interval.

means of the graphic screen and plotter of the Wang 2200 VP computer in such a way that low measuring data are associated with a light image area and the higher measuring data with a darker image area (Fig. 6A-C). To associate the twelve grey steps to all the measured data, the range, in which 99% of all measured GLIs are placed, is divided at twelve equidistant intervals and the GLIs of this interval are replaced by the corresponding step-element; larger GLI-data than that of the 99% level are replaced by the darkest step-element. For this purpose the distribution of the GLIs has to be determined previously.

Using a microscope with a drawing facility, the original section can be overlaid by the plotted image and the laminae can be transferred on to the data matrix. Here the row and column numbers can easily be counted and fed in to the computer. By marking significant structures (e.g. vessels) on the plotted image, the investigator can use the neighbouring fibre-stained sections as additional criteria for the demarcation of the laminae.

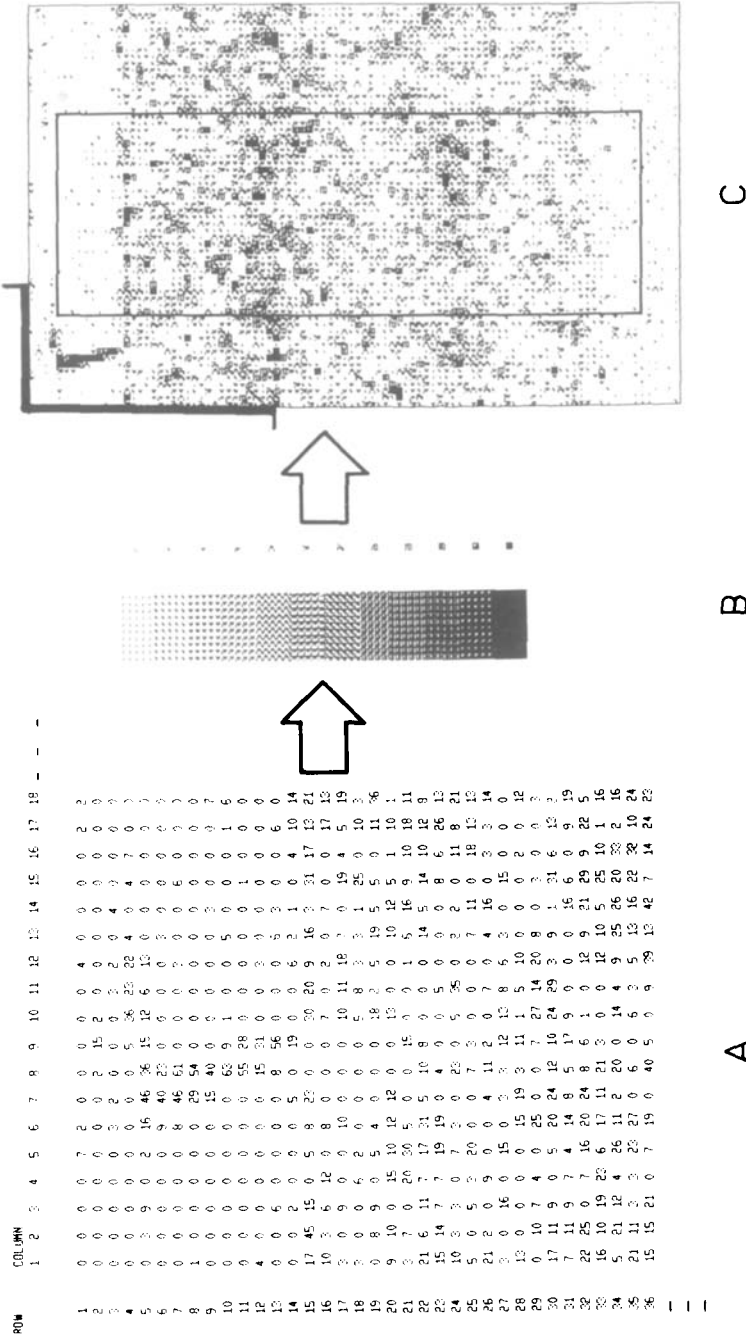


**Fig. 6.** (A) Data matrix corresponding to Fig. 2 (detail); (B) grey steps and elements; (C) plotted image corresponding to the data matrix in (A) and the photograph in Fig. 2. The data matrix part in (A) is indicated in the left upper part. The demarcated image-part will be used for the further analysis (measuring field: width 20  $\mu\text{m}$ , height 20  $\mu\text{m}$ ; analysed cortex part: width 60 measuring fields, height 96 measuring fields; GLI 1–36°, divided in twelve classes).



*GLI profile and data on the laminae*

A typical cortical profile is obtained by integrating the measured data of a row to a portion of the plotted image (Fig. 6C) delimited previously in the plotted image, which does not show any disturbing vascular structures or histological processing errors, and by plotting them against the row number. Such an absolute data profile, however, depends on several very important facts, which will not be discussed further in this report, i.e. the different shrinkage of the sections during histological process, which influences the *x*-axis of the absolute data profile; the depth of focus of the optical equipment, the GLI increases as the depth of focus becomes greater; and the grey level threshold-setting because there is a range of uncertainty which produces significant absolute but negligible relative alterations of the GLIs.

On the basis of these facts, it was decided to use only the relative GLI for quantitative analysis. Having made this decision, standardization must be developed. This standardization is carried out so that the area below the GLI profile as well as the thickness of the cortex are equal to 1, and thereby a considerably better comparison of different profiles can be made. Zilles & Schleicher (1980) used the same standardization for ontogenetic studies with the help of the GLI profile. For better orientation, the absolute scale of the *x*-axis is noted on the GLI profile (Fig. 7). Furthermore the profile is smoothed out to eliminate jumps in the profile which are of no significance. The smoothened total of row *i* ( $Z_i$ ) results from the row totals  $R_j$  according to the following formula:

$$Z_i = 0.1R_{i-2} + 0.6R_{i-1} + R_i + 0.6R_{i+1} + 0.1R_{i+2}$$

X-SCALE: 0 = EXTERNAL BOUNDARY OF THE CORTEX  
 1 = INNER BOUNDARY OF THE CORTEX EQUAL TO 1720 μm  
 EXTERNAL X-SCALE: 1 DIVISION = 100 μm  
 Y-SCALE: 0 = GREY LEVEL INDEX 0  
 1 = MEAN GREY LEVEL INDEX OF THE EVALUATED CORTEX PART EQUAL TO 6.2 %

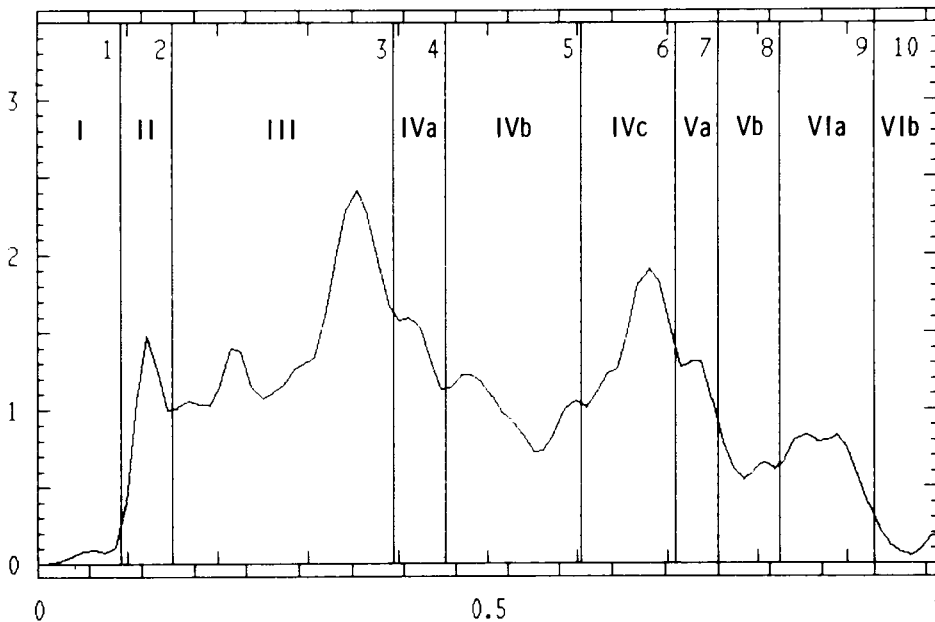


**Fig. 7.** Computer print with GLI profile corresponding to the demarcated image part in Fig. 6C (area and length standardized; mean GLI of a measuring field in the evaluated cortex part: 6.2%; thickness of the cortex: 1720 μm; smoothing factors: 0.1-0.6-1-0.6-0.1). The boundaries of ten laminae are plotted in the graph.

The boundaries of the laminae determined in the plotted image by the investigator and fed to the computer are immediately plotted into the GLI profile (Fig. 7).

The computer also produces a print (Fig. 8) which indicates data for every lamina. The data given in the print were not calculated using the data from the smoothed but from the unsmoothed rows. This was to obtain better selectivity between the single laminae, because such a procedure always smoothens sharp transitions, an effect which is required for profile representation, while for the computation it will only lead to unnecessary mistakes. The calculated data are stored in an external data file and can be used for further analysis.

LAMINA	I	NO. OF ROWS	I	ABS. THICKN.	I	REL. THICKN.	I	REL. PORTION	I	MEAN ABS. GLI	I	MEAN REL. GLI
I	I	5 - 12	I	160 $\mu\text{m}$	I	9.30 %	I	0.49 %	I	0.33 %	I	0.053
II	I	13 - 17	I	100 $\mu\text{m}$	I	5.81 %	I	6.18 %	I	6.60 %	I	1.064
III	I	18 - 38	I	420 $\mu\text{m}$	I	24.41 %	I	35.73 %	I	9.07 %	I	1.463
IVa	I	39 - 43	I	100 $\mu\text{m}$	I	5.81 %	I	8.25 %	I	8.80 %	I	1.420
IVb	I	44 - 56	I	260 $\mu\text{m}$	I	15.11 %	I	15.43 %	I	6.33 %	I	1.020
IVc	I	57 - 65	I	180 $\mu\text{m}$	I	10.46 %	I	15.52 %	I	9.19 %	I	1.483
Va	I	66 - 69	I	80 $\mu\text{m}$	I	4.65 %	I	5.59 %	I	7.45 %	I	1.202
Vb	I	70 - 75	I	120 $\mu\text{m}$	I	6.97 %	I	4.27 %	I	3.80 %	I	0.613
VIa	I	76 - 84	I	180 $\mu\text{m}$	I	10.46 %	I	7.66 %	I	4.54 %	I	0.732
VIb	I	85 - 90	I	120 $\mu\text{m}$	I	6.97 %	I	0.82 %	I	0.73 %	I	0.118

**Fig. 8.** Computer list of the fraction quotas of the evaluated laminae corresponding to the GLI profile in Fig. 7. The rows contain: (1) The number of rows which determine this lamina. They are counted on the plotted image and fed into the program. (2) The absolute thickness of this lamina in micrometres. (3) The relative thickness of this lamina in per cent. That is the thickness of the lamina in relation to the total thickness of the cortex at this point. (4) The relative portion of the GLI profiles in per cent. The area under the grey level index profile always has the value 1. The relative portion indicates which percentage of the total area under the curve is taken by the lamina in question. The relative portion can also be obtained by multiplying the relative thickness by the mean relative GLI of the lamina. (5) The mean absolute GLI of the lamina. This is the mean GLI of all GLIs in this lamina. (6) The mean relative GLI of a lamina. The obtained mean absolute GLI of a lamina is related to the mean absolute GLI of the whole cortex part evaluated.

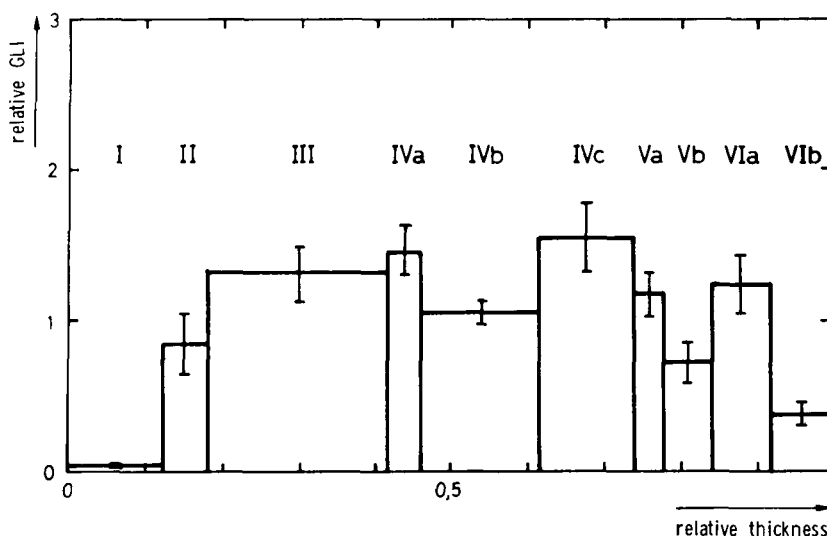
## RESULTS

Figure 9 shows the mean values for the relative thickness and relative GLI of the GLI profile obtained from averages within individuals. At 1.46 and 1.57, respectively, lamina IVa and IVc have the highest mean relative GLI. This corresponds with the general opinion that, in the striate area, the inner granular lamina (lamina IVc) has the highest cell density. The GLI of lamina IVb corresponds almost exactly with the mean GLI of the total striate area. With the exception of the two marginal laminae I and VIb, lamina Vb shows a remarkably low mean relative GLI of 0.72. This corresponds with the subjective impression gained when examining a cresyl-fast-violet stained section of the striate area (Fig. 2). Lamina Vb is to be seen as a very light stripe.

## DISCUSSION

Although the grey level of a microscopically visible cell is of great importance for the determination of the GLI, this method is quite different from photometric measuring (Ryzen, 1956). The GLI is a real area portion, the extinction defines the demarcation of the area. A photometric procedure only defines the extinction value of a measuring field which in cresyl-fast-violet stained sections must have an analogous connection with the density of stained particles of this field. Here, however, differences in staining which can never be avoided completely are a substantial source of error. In the GLI-method the influence of staining can be compensated by a fitted threshold setting.

Haug (1955, 1958) used a quantitative method which utilizes the so-called 'grey cell coefficient', the ratio of total volume to cell volume, as a measuring dimension. The grey cell coefficient can be determined by a point-counting method, in which only the well-focused cell-parts in the



**Fig. 9.** Profile of the mean GLIs of the laminae of the striate area. Bars indicate standard deviations between individuals.

image of a microscope are taken into account. The present method utilizing the GLI includes strong light-absorbing particles which are slightly out of focus. More recently, Haug (1979) developed a semi-automatic measuring method for evaluating layered tissue, in which the arrangement of measuring fields is similar to that used in this study. As the area of cells must be examined by planimetry using a magnetostrictive tableau and a cursor (MOP-System), this method is also very time-consuming. On the other hand, it results in quantitative information on the amount of nerve-cells and glia-cells and on nerve-cell-size-distribution in the different cell-layers of the cerebral cortex.

Although glia and nerve cells cannot be differentiated by the GLI-method and only relative GLI data related to the mean GLI of the whole analysed cortex part are examined, this procedure does offer a considerable advantage in that it is extremely time-saving in contrast to the non-automatic measurements used by Haug. Unfortunately, however, this saving of time also results in loss of information.

To compare the relative proportions of the thickness of the laminae in the striate area, the data of four publications were used (Table 1). The present data on laminae I, II, Va-VIb correspond quite well with those of other publications. Only the values for lamina VI of LeRoy Conel (1967) and Filimonoff (1929) are considerably higher. LeRoy Conel examined a non-adult brain which may show positive differences from an adult brain. Since Filimonoff obtained his results from a single measurement, the difference can be explained by the great variability of the cortex. Just the inner laminae of the tops of the vaults can be tremendously thick (Bok, 1929).

The values given by v. Economo & Koskinas (1925) and Filimonoff (1929) for lamina IVa are higher than those found in the present study. On the other hand, the present data for lamina III are correspondingly higher so that the sums of III and IVa are in accordance with one another. This difference can be explained by variations in the boundary setting between laminae III and IVa. v. Economo & Koskinas (1925) fixed this boundary at the point where an evident increase in density in lamina III is to be seen. This boundary does not correspond with the one used in the present examinations. This boundary between III and IVa is mostly situated beyond the increase in density (Sauer, 1982). A similar explanation can be given for the differences seen for laminae IVb and IVc.

As the grey level index offers a new measurement value for quantitative estimations of the cortex, no directly comparable data on the cortical laminae are to be found in other publications.

**Table 1.** Comparison of the relative thickness of the laminae of the striate area published by different authors. *v. Economo & Koskinas* (1925) published data on the different positions of the cortical convolution (top, wall of convolution, etc.). For comparison only the two values for the wall of convolution were included, because in this area, the laminae are generally only minimally influenced by the fold. The data of *Filimonoff* (1929) were obtained from the striate area of the brain of a 30-year-old male. *Haug* (1958) gave findings from twenty different brains and thus the mean values were used for comparison. The findings of *LeRoy Conel* (1967) were obtained from the brain of a 6-year-old child. When the publications only gave absolute values, the relative values were calculated.

Lamina	Relative thickness (%)					
	<i>v. Economo &amp; Koskinas</i> (1925)	<i>Filimonoff</i> (1929)	<i>Haug</i> (1958)	<i>LeRoy Conel</i> (1967)	<i>Sauer</i>	
I	9.5 13.0	8.8	12.4	11.5	11.2	
II	5.7	5.4	}	5.1	6.0	
III	9.8 12.4 20.7	15.1		32.9	17.8	23.6
IVa	9.5 8.7	7.3	}	}	5.0	
IVb	13.3 13.0	12.2			13.4	15.0
IVc	16.2 14.1	15.1			15.4	12.6
Va	}	}	}	}	4.2	
Vb					11.4 7.6	9.7
VIa	12.4	17.1	9.2	}	8.0	
VIb	7.6 9.5 5.4	9.3	8.6		32.0	8.1

**Table 2.** Comparison between the relative reciprocal grey cell coefficient and the GLI of the laminae of the striate area.

Lamina	Relative reciprocal grey cell coefficient ( <i>Haug</i> , 1958)		Relative grey level index	
	Mean value of twenty cases	Standard deviation	Mean value of eleven cases	Standard deviation
I	0.07	0.024	0.04	0.014
II + III + IVa	1.29	0.094	1.24	0.169
IVb	0.83	0.091	1.05	0.083
IVc	1.35	0.095	1.57	0.230
V	0.81	0.066	0.89	0.120
VIa	1.54	0.127	1.25	0.195
VIb	0.54	0.078	0.39	0.103

*Haug*, however, described extensive quantitative examinations of the striate area using the grey cell coefficient. Since there is a considerable difference in definition and method between the grey cell coefficient and the GLI, only a comparison based on the results of measurements is to be attempted. Therefore the present results have to be converted into the lamina classification of *Haug*, i.e. laminae II, III and IVa as well as laminae Va and Vb must be combined. The grey cell coefficient has to be converted into its reciprocal value and must be standardized with the total grey cell coefficient. The mean values of the different laminae of normal adult brains which result from this procedure are shown in Table 2 with their standard deviations.

In summary, it can be said that, despite the differences in method, the relative GLI and reciprocal relative grey cell coefficient produce similar, partially well-corresponding data for the individual laminae of the striate area.

## ACKNOWLEDGMENTS

This work was supported by the Stiftung Volkswagenwerk (Grant I/34235). The author wishes to thank Miss Dipl.-Inf. Krauthausen, Mr Dipl.-Math. Herrmann and Dr Lange for their critical advice and Miss Hamilton and Miss Markmann for translating and typing the manuscript. Special thanks are due to Professor Dr Rabl for providing us with the histological material and Professor Dr Kretschmann who supported all phases of this study.

## REFERENCES

- Bok, S.T. (1929) Der Einfluss der in den Furchen und Windungen auftretenden Krümmungen der Grosshirnrinde auf die Rindenarchitektur. *Z. ges. Neurol. Psychiat.* **121**, 682.
- Economo, C. v. & Koskinas, G.N. (1925) *Die Cytoarchitektonik der Hirnrinde des erwachsenen Menschen*. Springer, Wien.
- Filimonoff, I.N. (1929) Zur embryonalen und postembryonalen Entwicklung der Grosshirnrinde des Menschen. *J. Psychol. Neurol. (Lpz.)*, **39**, 323.
- Haug, H. (1955) Die Treffermethode, ein Verfahren zur quantitativen Analyse im histologischen Schnitt. *Z. Anat. Entwickl.-Gesch.* **118**, 302.
- Haug, H. (1958) *Quantitative Untersuchungen an der Sehrinde*. Thieme, Stuttgart.
- Haug, H. (1979) The evaluation of cell-densities and of nerve-cell-size distribution by stereological procedures in a layered tissue (cortex cerebri). *Microsc. Acta*, **82**, 147.
- LeRoy Conel, J. (1967) *The Postnatal Development of the Human Cerebral Cortex*, Vol. 8. *The Cortex of the Six-Year Child*. Harvard University Press, Massachusetts.
- Robertson, A.J., Anderson, J.M., Brown, R.A., Slidders, W. & Swanson Beck, J. (1978) Grading of astrocytomas using a Quantimet 720 image-analysing computer. *J. clin. Path.* **31**, 469.
- Ryzen, M. (1956) A microphotometric method of cell enumeration within the cerebral cortex of man. *J. comp. Neurol.* **104**, 233.
- Sauer, B. (1982) Lamina boundaries of the human striate area compared with automatically obtained grey level index profiles. *J. Hirnforsch.* (in press).
- Schleicher, A., Zilles, K. & Kretschmann, H.-J. (1978) Automatische Registrierung und Auswertung eines Grauwertindex in histologischen Schnitten. *Verh. anat. Ges. (Jena)*, **72**, 413.
- Tucker, J.H. (1979) An image analysis system for cervical cytology automation using nuclear DNA content. *J. Histochem. Cytochem.* **27**, 613.
- Wied, G.L., Bartels, P.H., Bibbo, M., Puls, J., Taylor, J. & Sychra, J.J. (1978) Computer recognition of ectocervical cells classification accuracy and spatial resolution. *Acta Cytol.* **21**, 753.
- Zilles, K. & Schleicher, A. (1980) Quantitative Analyse der laminären Struktur menschlicher Cortexareale. *Verh. Anat. Ges.* **74**, 725.
- Zilles, K., Schleicher, A. & Kretschmann, H.-J. (1978) A quantitative approach to cytoarchitectonics. I. The areal pattern of the cortex of *Tupaia belangeri*. *Anat. Embryol.* **153**, 195.
- Zilles, K., Zilles, B. & Schleicher, A. (1980) A quantitative approach to cytoarchitectonics. VI. The areal pattern of the cortex of the albino rat. *Anat. Embryol.* **159**, 335.